

## Enhanced energy-storage performance of 0.94NBT-0.06BT thin films induced by a $Pb_{0.8}La_{0.1}Ca_{0.1}Ti_{0.975}O_3$ seed layer



Y.L. Zhang<sup>a</sup>, W.L. Li<sup>a,b,\*</sup>, W.P. Cao<sup>a</sup>, T.D. Zhang<sup>a</sup>, T.R.G.L. Bai<sup>a</sup>, Y. Yu<sup>a</sup>, Y.F. Hou<sup>a</sup>, Y. Feng<sup>a</sup>, W.D. Fei<sup>a</sup>

<sup>a</sup> School of Materials Science and Engineering, Harbin Institute of Technology, Harbin 150001, PR China

<sup>b</sup> National Key Laboratory of Science and Technology on Precision Heat Processing of Metals, Harbin Institute of Technology, Harbin 150001, PR China

### ARTICLE INFO

#### Article history:

Received 25 April 2016

Received in revised form

6 June 2016

Accepted 17 June 2016

Available online 18 June 2016

#### Keywords:

NBT-BT thin films

Sol-gel process

Energy-storage

### ABSTRACT

0.94( $Na_{0.5}Bi_{0.5}TiO_3$ )-0.06BaTiO<sub>3</sub> ferroelectric thin films with and without the  $Pb_{0.8}La_{0.1}Ca_{0.1}Ti_{0.975}O_3$  seed layer were deposited on platinum-buffered silicon substrates by using Sol-Gel process. The influence of  $Pb_{0.8}La_{0.1}Ca_{0.1}Ti_{0.975}O_3$  seed layer and annealing temperatures on the microstructures, ferroelectric properties and energy-storage performances of the as-prepared films were investigated in details. The low annealing temperature and  $Pb_{0.8}La_{0.1}Ca_{0.1}Ti_{0.975}O_3$  seed layer could improve the values of electric break-down field strength and  $P_{max}-P_r$ , which play a vital role for high recoverable energy-storage density. Owing to the high electric break-down field strength value of 3310 kV/cm, a large recoverable energy density of  $W=17.2\text{ J/cm}^3$  and a high energy efficiency of  $\eta=74.3\%$  were obtained for the 0.94 ( $Na_{0.5}Bi_{0.5}TiO_3$ )-0.06BaTiO<sub>3</sub> thin film with the  $Pb_{0.8}La_{0.1}Ca_{0.1}Ti_{0.975}O_3$  seed layer, which was annealed at 450 °C.

© 2016 Elsevier Ltd and Techna Group S.r.l. All rights reserved.

## 1. Introduction

In recent years, with the development of pulse-power-technology and micro-electronics technology, dielectric materials with high-energy storage density, fast charge/discharge, low cost, and good temperature stability are urgently needed for the potential application in advanced capacitors [1–6]. Commonly, the recoverable energy storage density  $W$  could be estimated from the following equation:

$$W = \int_{P_r}^{P_{max}} EdP \quad (1)$$

where  $E$  is the applied electric field,  $P$  is the polarization,  $P_{max}$  is the maximum saturated polarization and  $P_r$  is the remnant polarization. Considering the equation above, it could be predicted that dielectric materials with a large difference between  $P_{max}$  and  $P_r$  and high electric break-down field strength (BDS) should be potential candidates for high recoverable energy-storage applications [7–9]. Up to now, the reported works on energy-storage materials were mainly focused on bulk ceramics. Because of the lower breakdown field, the energy-storage density of the bulk ceramics is usually very small [10]. For example, it was reported

that the maximum recoverable energy-storage density in 0.89 ( $Na_{0.5}Bi_{0.5}TiO_3$ )-0.06BaTiO<sub>3</sub>-0.05( $K_{0.5}Na_{0.5}$ )NbO<sub>3</sub> ceramics was only 0.59 J/cm<sup>3</sup> [11]. Comparatively, thin films possess high break-down strength, they could conquer the shortcomings in bulk ceramic and be suitable for the application in high energy-storage capacitors. A large recoverable  $W$  value of 31.3 J/cm<sup>3</sup> was achieved in 0.9Pb(Mg<sub>1/3</sub>Nb<sub>2/3</sub>)O<sub>3</sub>-0.1PbTiO<sub>3</sub> relaxor ferroelectric thin films [12]. To date, the most studied energy-storage materials are lead-based. However, lead-containing materials are considered to be a serious threat to the environment and human health. Thus the investigations on lead-free energy-storage materials are gradually attracting researches' attention.

$Na_{0.5}Bi_{0.5}TiO_3$  (NBT) with 1:1 ratio of  $Na^+$  and  $Bi^{3+}$  at A-site is a typical perovskite-type lead-free ferroelectric at room temperature and displays an relaxor ferroelectric behavior at high temperature of above 220 °C [13,14].  $Bi^{3+}$  has the electronic configuration similar to  $Pb^{2+}$  in PbTiO<sub>3</sub>, which causes high polarization (as in lead-based materials) due to the existence of stereo-chemically active lone pair electrics [15,16]. In order to improve the properties of NBT,  $Ba^{2+}$ ,  $Sr^{2+}$ ,  $Ca^{2+}$ , etc. have been doped to NBT. Among the NBT-based solutions, (1-x)( $Na_{0.5}Bi_{0.5}TiO_3$ -xBaTiO<sub>3</sub>) ((1-x)NBT-xBT) system has attracted much attention due to its morphotropic phase boundary (MPB) between rhombohedral and tetragonal phases at  $x=0.06$ , which allows a significant improvement of their dielectric, ferroelectric and piezoelectric properties [17,18]. It was found that the addition of BT could enhance the values of BDS and  $P_{max}-P_r$  at the same time. The energy-storage

\* Corresponding author at: School of Materials Science and Engineering, Harbin Institute of Technology, Harbin 150001, PR China.

E-mail address: [wlli@hit.edu.cn](mailto:wlli@hit.edu.cn) (W.L. Li).

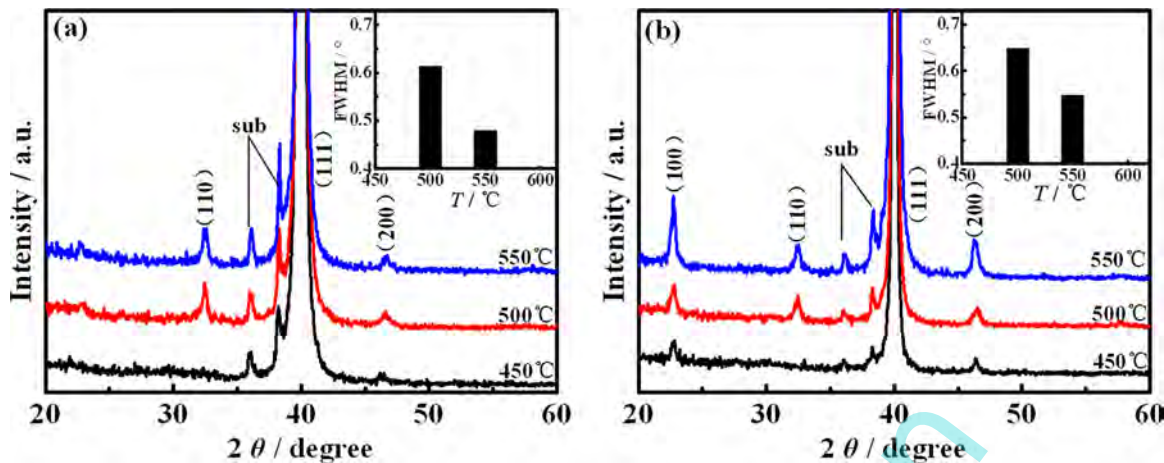


**Fig. 1.** XRD patterns of (a) 0.94NBT-0.06BT thin film and (b) 0.94NBT-0.06BT thin film with PLCT seed layer annealed at different temperatures.

performances of  $\text{Bi}_2\text{O}_3\text{-Li}_2\text{O}$  added 0.94NBT-0.06BT films were studied by Zhang et al., and a maximum  $W=2.3 \text{ J/cm}^3$  at 550 kV/cm was obtained [19].

The volatile elements in NBT-based solutions will be volatile during the thermal treatment, which induces oxygen vacancies to maintain charge neutrality in the lattice. As a result, the material's conductivity enlarged and ferroelectric property deteriorated [20]. Especially for the NBT-based thin film, the leakage problem is more severe and it may hinder its future applications in devices. Feng and his coauthors reported the leakage current of  $\text{Na}_{0.5}\text{Bi}_{0.5}\text{Ti}_{0.98}\text{Mn}_{0.02}\text{O}_3$  thin film, which shows a decreasing tendency at the low annealing temperature [15]. It has been demonstrated that decreasing annealing temperature can reduce volatilization in thin film with volatile elements which would induce the formation of oxygen vacancies [21,22]. Chi et al. introduced the  $\text{Pb}_{0.8}\text{La}_{0.1}\text{Ca}_{0.1}\text{Ti}_{0.975}\text{O}_3$ (PLCT) seed layer between  $(\text{Na}_{0.85}\text{K}_{0.15})_{0.5}\text{Bi}_{0.5}\text{TiO}_3$  films and the electrode, the PLCT seed layer favored the grain growth and reduced the leakage current [23]. The aim of the PLCT seed layer is to decrease the crystallization temperature and reduce interfacial diffusion [24], then the quality of films is improved and the leakage current is decreased [25].

Therefore, in this paper, 0.94NBT-0.06T thin films were fabricated by Sol-Gel method and annealed at different temperatures temperature. The PLCT seed layer was introduced at the interface between the 0.94NBT-0.06BT thin films and the substrates in an attempt to enhance the energy storage performance.

## 2. Experimental procedure

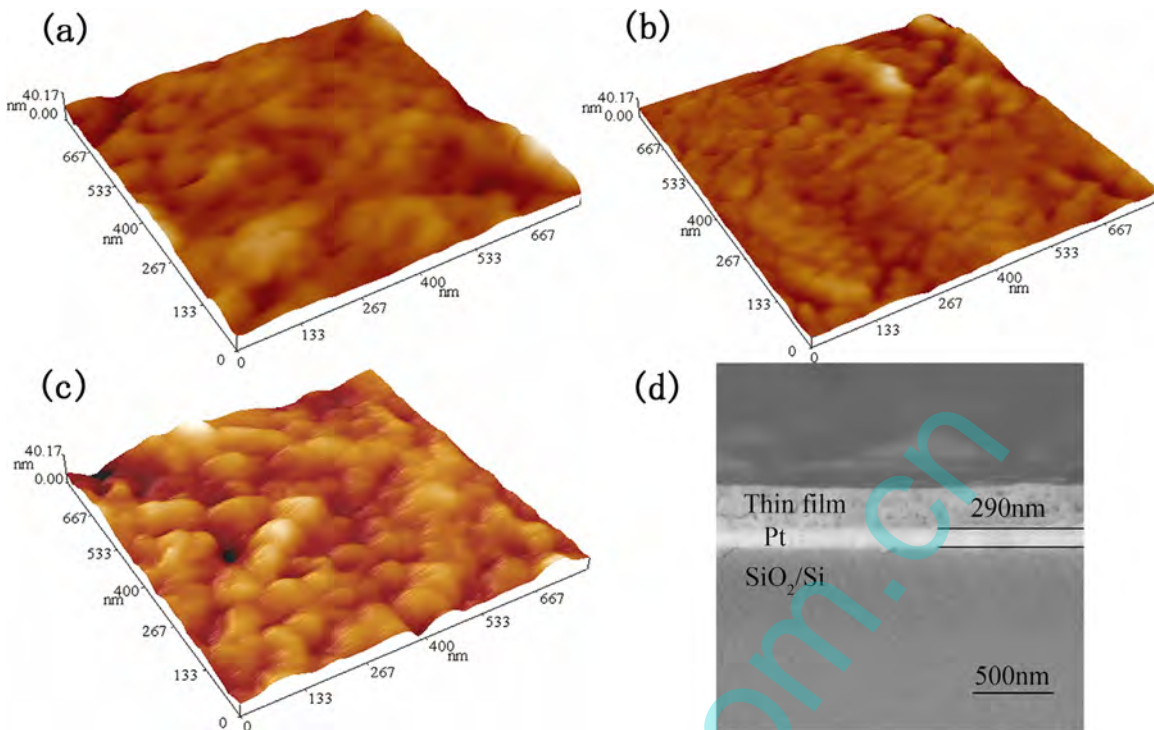
0.94NBT-0.06BT thin films were prepared by Sol-Gel method. Bismuth nitrate pentahydrate, sodium acetate, tetrabutyl titanate and barium acetate were selected as the raw materials. 2-Methoxyethanol and acetylacetone were used as the solvent and the chelating agent and Glycerol were used as stabilizers, respectively. 10 mol% excess of sodium acetate and 5 mol% excess of bismuth nitrate pentahydrate were introduced to compensate the evaporation of sodium and bismuth during high-temperature annealing process. The concentration of the precursor solution was adjusted to 0.3 M. The PLCT thin film was deposited by Sol-Gel spin-on technique, lead acetate trihydrate, lanthanum acetate hydrate, calcium acetate and tetrabutyl titanate were used as the raw materials and 2-methoxyethanol as the solvent. The 10 mol% excess of Pb solution was used to over compensate for any Pb loss during high temperature annealing, the composition of the solution was controlled to in the ratio of  $\text{Pb:La:Ca:Ti}=0.8:0.1:0.1:0.975$ , the concentration of the PLCT sol was adjusted to 0.1 M. Firstly, a thin PLCT layer was deposited on a Pt/Ti/SiO<sub>2</sub>/Si substrate and pyrolyzed on a hotplate at

350 °C for 5 min. Then the films were annealed at 650 °C. Secondly, the NBT-BT layers were deposited on the PLCT coating and pyrolyzed at 400 °C for 5 min repeatedly until the desired film thickness was achieved. Finally, the films were respectively annealed at 450 °C, 500 °C and 550 °C for 5 min respectively by rapid thermal annealing (RTA, the heating rate is 60 °C) in an oxygen atmosphere. The phase purity and crystal structure were examined by X-ray diffraction (XRD) using a Philips X'Pert diffractometer with CuK $\alpha$  radiation operated at 40 kV and 40 mA. The surface and cross-sectional morphologies of thin films were observed by atomic force microscopy (CSPM5600 of Benyuan) and scanning electron microscopy (Helios Nanolab600i), respectively. To measure the ferroelectric properties of the films, dot-type Pt electrodes with an area of  $3.14 \times 10^{-4} \text{ cm}^2$  were deposited on each NBT-BT film by magnetron sputtering. Ferroelectric properties and leakage current characteristics were evaluated using a Radian Technologies Precision workstation ferroelectric measurement system.

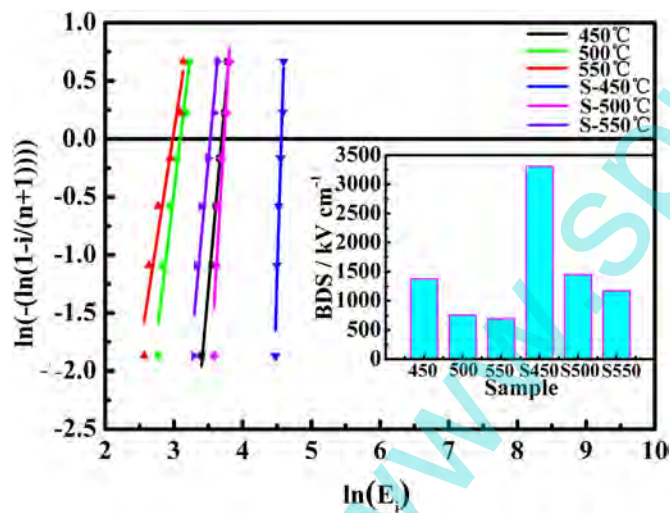
## 3. Results and discussion

Fig. 1 shows the XRD patterns of 0.94NBT-0.06BT thin films with and without the PLCT seed layer formed at different annealing temperatures (450, 500 and 550 °C). Pure 0.94NBT-0.06BT thin film annealing at 450 °C is incompletely crystallized. The other thin films exhibit a pure perovskite phase without any secondary phase peaks, and the addition of the PLCT seed layer reduces crystallization temperature. All the thin films exhibit random orientation. With increasing annealing temperatures, the intensities of (100) and (200) peaks of the 0.94NBT-0.06BT thin film with the PLCT seed layer (0.94NBT-0.06BT/PLCT) increase significantly. The inset illustrates the full width at half maximum (FWHM) of the (110) peak for these thin films. The values of the FWHM decrease with the increasing annealing temperature, implying the average grain size increases with the increasing annealing temperature [7].

Fig. 2(a)–(c) show the surface micrographs of 0.94NBT-0.06BT/PLCT thin films annealed at 450, 500 and 550 °C, respectively. The cross-section image of the 0.94NBT-0.06BT thin film with the PLCT seed layer annealed at 450 °C is given in Fig. 2(d) as a typical example. From the surface micrographs (Fig. 2(a)–(c)), it can be observed that all the samples exhibit a uniform and dense surface structure and the grain size of the 0.94NBT-0.06BT/PLCT thin film annealed at 550 °C is largest. The surface roughness of 0.94NBT-0.06BT/PLCT thin films annealed at 450, 500 and 550 °C are 2.89, 4.65 and 4.73 nm, respectively. It can be seen that the surface roughness increases with the increasing annealing temperature. The thickness of the film is about 290 nm, determined from the



**Fig. 2.** (a)–(c) The surface micrographs of 0.94NBT-0.06BT/PLCT thin films annealed at 450, 500 and 550 °C and (d) SEM cross profile images of the 0.94NBT-0.06BT thin films with PLCT seed layer annealed at 450 °C.



**Fig. 3.** Weibull distributions and the fitting lines of BDS of all the samples.

cross-section picture. No obvious inter-diffusion between thin film and Pt bottom electrode is detected and no preferential orientation is found in the investigation. Considering that the PLCT seed layer is too thin, so the thickness of the all the 0.94NBT-0.06BT thin films is about 290 nm.

Fig. 3 depicts Weibull distribution of BDS for the 0.94NBT-0.06BT thin films. The values of BDS can be described by:

$$X_i = \ln(E_i) \quad (2)$$

$$Y_i = \ln\left(-\left(\ln\left(1 - \frac{i}{n+1}\right)\right)\right) \quad (3)$$

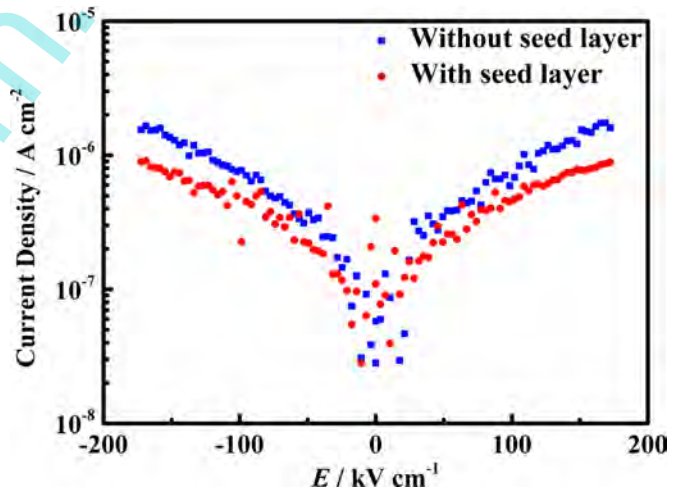


**Fig. 4.** Leakage current characteristics of 0.94NBT-0.06BT thin films without and with seed layer, which were annealed at 450 °C.

where  $X_i$  and  $Y_i$  are the two parameters in Weibull distribution function,  $i$  is the serial number of the samples ( $i=1, 2, \dots$ ), and  $n$  is the sum of specimens of each sample.  $E_i$  is the specific breakdown voltage of each specimen in the experiments, and  $E_i$  is arranged in ascending order of  $E_1 < E_2 < E_3 < \dots < E_n$ . According to Weibull distribution function,  $X_i$  and  $Y_i$  have a linear relationship. The mean BDS could be extracted from the points where the fitting lines intersect with the horizontal line through  $Y_i=0$ .

According to the data given in the Fig. 3, pure 0.94NBT-0.06BT thin films annealed in low temperature have a higher BDS, with the increase of annealing temperature BDS value reduced. This phenomenon is also found in 0.94NBT-0.06BT thin films with PLCT seed layer. The biggest BDS value obtained from the X intercept of the fitting lines is 3310 kV/cm in 0.94NBT-0.06BT/PLCT annealed at 450 °C. It is not hard to find that the films with the PLCT seed layer

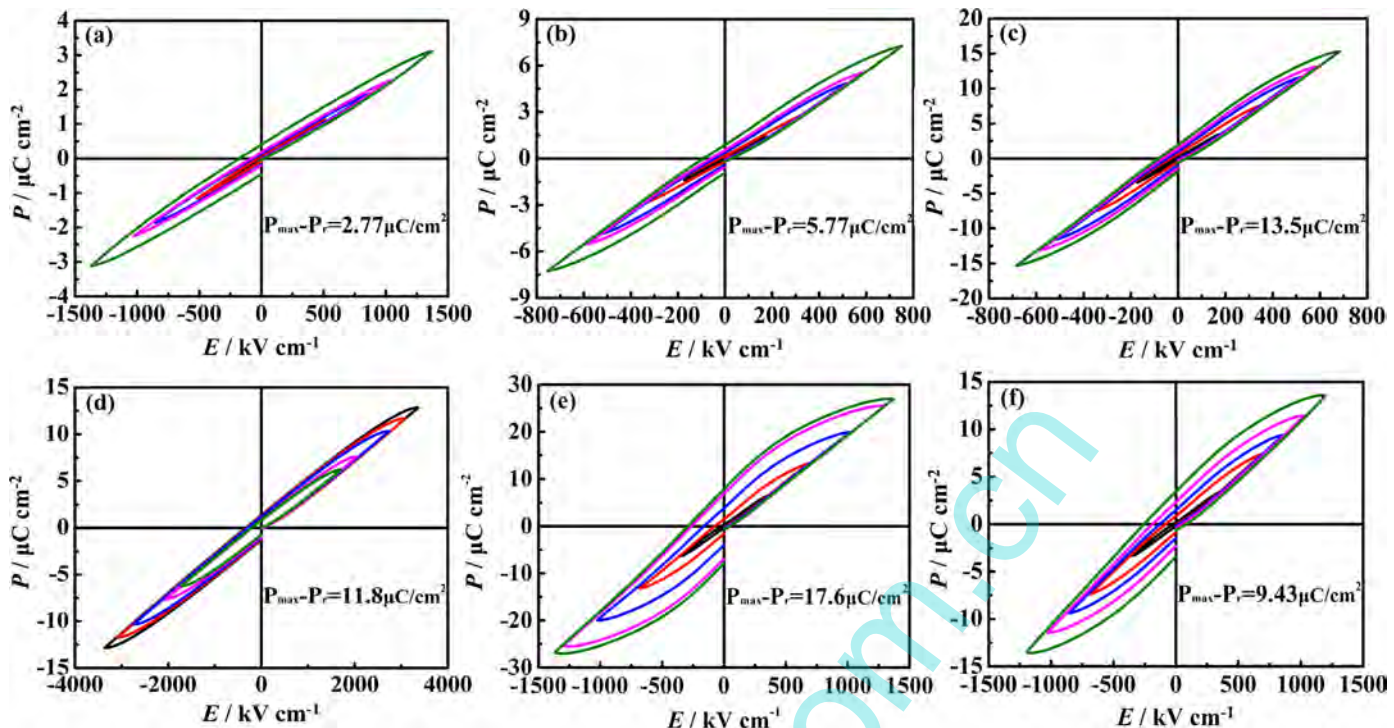


Fig. 5. P-E loops of (a-c) pure 0.94NBT-0.06BT thin films annealed at 450, 500, 550 °C and (d, e) 0.94NBT-0.06BT thin films with PLCT seed layer annealed at 450, 500, 550 °C.

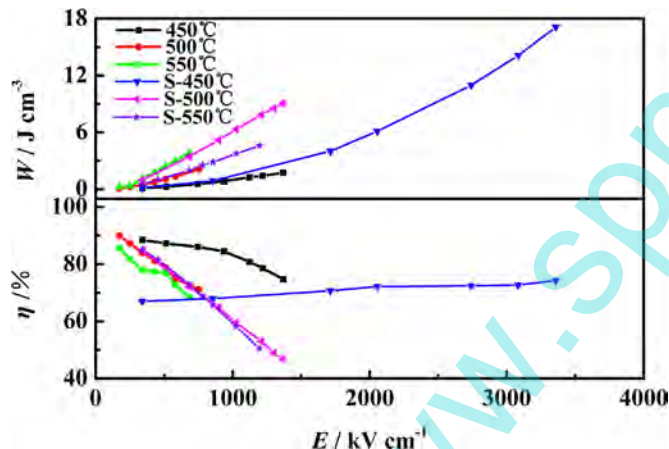


Fig. 6. The recoverable energy density  $W$  and energy-storage efficiency  $\eta$  of all samples.

have a higher BDS compared with pure 0.94NBT-0.06BT thin films at the same annealing temperature. The low annealing temperature and the PLCT seed layer are the main reason that leads to higher BDS. Because of the low annealing temperature reduces the density of oxygen vacancies and defect complexes in the film, the seed layer of the PLCT can favor the grain growth, decrease the crystallization temperature and block the spread between the base and thin film.

Fig. 4 depicts the curve of leakage current density versus electric field  $E$  behavior of 0.94NBT-0.06BT thin films with and without seed layer, which were annealed at 450 °C. The results show that the leakage current densities have obvious differences. Compared with pure 0.94NBT-0.06BT thin film, the film with the PLCT seed layer has lower current densities comparing, which leads to a high BDS. The PLCT seed layer reduced the leakage current and improved the quality of thin film. It is consistent with the results of Fig. 3.

As is mentioned earlier, energy storage density is not only

related with the BDS but also with related to value of  $P_{max}-P_r$ . Dielectric materials with large value of  $P_{max}-P_r$  and high electric breakdown field strength (BDS) could have high recoverable energy-storage density. To further investigate the influence of electric-field-strength dependence on the energy storage, the room temperature P-E loops under different electric fields of the samples are discussed and are shown in Fig. 5, which were measured at 1 kHz. The  $P_{max}-P_r$  values of all of the samples were measured at their critical breakdown strength. 0.94NBT-0.06BT thin films with and without the PLCT seed layer which were annealed at 450 °C have a small remnant polarization, and  $P_r$  changes little with increasing electric field,  $P_{max}$  clearly increases with increasing electric field, this is helpful to obtain larger  $P_{max}-P_r$ . For pure 0.94NBT-0.06BT thin films, leakage current increases with increasing annealing temperature. Compared with pure 0.94NBT-0.06BT thin films, the films with seed layer have a higher  $P_{max}-P_r$ . The biggest  $P_{max}-P_r$  value is 17.6  $\mu\text{C}/\text{cm}^2$  for the 0.94NBT-0.06BT/PLCT thin film annealed at 500 °C.

Fig. 6 illustrates the energy-storage density  $W$  and energy-storage efficiency ( $\eta$ ) of 0.94NBT-0.06BT thin films. As is desired, with the electric field increasing, the  $W$  values of all the thin films increase linearly. For pure 0.94NBT-0.06BT thin films, the energy-storage density  $W$  which measured at its BDS, the values of  $W$  reduce with increasing annealing temperature, which is due to the decrease of  $P_{max}-P_r$  with increasing annealing temperature. It could be easily found that the  $W$  values of seed layer-added samples have improved a lot compared with pure 0.94NBT-0.06BT thin films. With the same annealing temperature, the film with PLCT seed layer has a higher energy storage density, which illustrates that the seed layer can improve the energy storage density. The maximum  $W$  values at their corresponding BDS are 17.2  $\text{J}/\text{cm}^3$  for the 0.94NBT-0.06BT/PLCT thin film annealed at 450 °C, which is due to its highest BDS and the higher  $P_{max}-P_r$  among all the samples. Up to now, this energy-storage density is higher than the previously reported value of lead-free films. Different from  $W$  values,  $\eta$  of all thin films declined with increasing electric field

except for 0.94NBT-0.06BT/PLCT thin film annealed at 450 °C because of the higher values of energy loss density at high electric fields. The  $\eta$  of the 0.94NBT-0.06BT/PLCT thin film which were annealed at 450 °C increases with increasing electric fields, and at its BDS the value of  $\eta$  is 74.3%, illustrating that energy loss density increases little with increasing electric fields.

#### 4. Conclusions

In summary, lead-free 0.94NBT-0.06BT thin films with and without PLCT seed layers were deposited on Pt/Ti/SiO<sub>2</sub>/Si substrates via the Sol-Gel method. It could be obtained from XRD results that the 0.94NBT-0.06BT thin film with PLCT seed layers was fully crystallized after annealing at 450 °C, while the 0.94NBT-0.06BT thin film without the seed layer was incompletely crystallized under the same conditions. The low annealing temperature and PLCT seed layers could improve the values of BDS and the differences between  $P_{\max}$  and  $P_r$ , which play a vital role for high recoverable energy-storage density. Owing to the high BDS value of 3310 kV/cm, a large recoverable energy density of  $W=17.2 \text{ J/cm}^3$  and a high energy efficiency of  $\eta=74.3\%$  were obtained for the 0.94NBT-0.06BT thin film with the PLCT seed layer, which was annealed at 450 °C. These results indicate that the 0.94NBT-0.06BT/PLCT thin film annealed at low temperature is promising for the application of advanced capacitors with high-energy storage density and efficiency.

#### Acknowledgements

This work was supported by the National Natural Science Foundation of China (Grant nos. 11272102 and 51471057).

#### References

- [1] A. Chauhan, S. Patel, R. Vaish, Mechanical confinement for improved energy storage density in BNT-BT-KNN lead-free ceramic capacitors, *AIP Adv.* 4 (2014) 087106.
- [2] T.M. Correia, et al., A lead-free and high-energy density ceramic for energy storage applications, *J. Am. Ceram. Soc.* 96 (2013) 2699–2702.
- [3] P.J. Hall, et al., Energy storage in electrochemical capacitors: designing functional materials to improve performance, *Energy Environ. Sci.* 3 (2010) 1238.
- [4] X. Hao, et al., Composition-dependent dielectric and energy-storage properties of (Pb,La)(Zr,Sn,Ti)O<sub>3</sub> antiferroelectric thick films, *Appl. Phys. Lett.* 102 (2013) 163903.
- [5] B. Peng, et al., Giant electric energy density in epitaxial lead-free thin films with coexistence of ferroelectrics and antiferroelectrics, *Adv. Electron. Mater.* 1 (2015) 1500052.
- [6] T. Wang, et al., Relaxor ferroelectric BaTiO<sub>3</sub>-Bi(Mg<sub>2/3</sub>Nb<sub>1/3</sub>)O<sub>3</sub> ceramics for energy storage application, *J. Am. Ceram. Soc.* 98 (2015) 559–566.
- [7] W. Cao, W. Li, High-energy storage density and efficiency of (1-x)[0.94 NBT-0.06 BT]-xST lead-free ceramics, *Energy Technol.* 3 (2015) 1198–1204.
- [8] M. Chandrasekhar, P. Kumar, Synthesis and characterizations of BNT-BT and BNT-BT-KNN ceramics for actuator and energy storage applications, *Ceram. Int.* 41 (2015) 5574–5580.
- [9] Z. Xu, X. Hao, S. An, Dielectric properties and energy-storage performance of (Na<sub>0.5</sub>Bi<sub>0.5</sub>)TiO<sub>3</sub>-SrTiO<sub>3</sub> thick films derived from polyvinylpyrrolidone-modified chemical solution, *J. Alloy. Compd.* 639 (2015) 387–392.
- [10] Y. Zhao, X. Hao, M. Li, Dielectric properties and energy-storage performance of (Na<sub>0.5</sub>Bi<sub>0.5</sub>)TiO<sub>3</sub> thick films, *J. Alloy. Compd.* 601 (2014) 112–115.
- [11] F. Gao, et al., Energy-storage properties of 0.89Bi<sub>0.5</sub>Na<sub>0.5</sub>TiO<sub>3</sub>-0.06BaTiO<sub>3</sub>-0.05K<sub>0.5</sub>Na<sub>0.5</sub>Nb<sub>3</sub> lead-free anti-ferroelectric ceramics, *J. Am. Ceram. Soc.* 94 (2011) 4382–4386.
- [12] X. Wang, et al., High energy-storage performance of 0.9Pb(Mg<sub>1/3</sub>Nb<sub>2/3</sub>)O<sub>3</sub>-0.1PbTiO<sub>3</sub> relaxor ferroelectric thin films prepared by RF magnetron sputtering, *Mater. Res. Bull.* 65 (2015) 73–79.
- [13] S. Quignon, et al., Synthesis and electrical properties of sputtered (Na<sub>0.5</sub>Bi<sub>0.5</sub>)TiO<sub>3</sub> thin films on silicon substrate, *J. Am. Ceram. Soc.* 95 (2012) 3180–3184.
- [14] J. Xu, et al., Ferroelectric and non-linear dielectric characteristics of Bi<sub>0.5</sub>Na<sub>0.5</sub>TiO<sub>3</sub> thin films deposited via a metalorganic decomposition process, *J. Appl. Phys.* 104 (2008) 116101.
- [15] C. Feng, et al., Reduced leakage current and large polarization of Na<sub>0.5</sub>Bi<sub>0.5</sub>Ti<sub>0.98</sub>Mn<sub>0.02</sub>O<sub>3</sub> thin film annealed at low temperature, *Ceram. Int.* 41 (2015) 14179–14183.
- [16] L. Zhang, X. Hao, Dielectric properties and energy-storage performances of (1-x)(Na<sub>0.5</sub>Bi<sub>0.5</sub>)TiO<sub>3</sub>-xSrTiO<sub>3</sub> thick films prepared by screen printing technique, *J. Alloy. Compd.* 586 (2014) 674–678.
- [17] A. Andrei, N.D. Scarisoreanu, Pulsed laser deposition of lead-free (Na<sub>0.5</sub>Bi<sub>0.5</sub>)<sub>1-x</sub>Ba<sub>x</sub>TiO<sub>3</sub> ferroelectric thin films with enhanced dielectric properties, *Appl. Surf. Sci.* 278 (2013) 162–165.
- [18] M. Rawat, K.L. Yadav, Structural, dielectric and ferroelectric properties of Ba<sub>1-x</sub>(Bi<sub>0.5</sub>Na<sub>0.5</sub>)<sub>x</sub>TiO<sub>3</sub> ceramics, *Ceram. Int.* 39 (2013) 3627–3633.
- [19] L. Zhang, X. Hao, L. Zhang, Enhanced energy-storage performances of Bi<sub>2</sub>O<sub>3</sub>-Li<sub>2</sub>O added (1-x)(Na<sub>0.5</sub>Bi<sub>0.5</sub>)TiO<sub>3</sub>-xBaTiO<sub>3</sub> thick films, *Ceram. Int.* 40 (2014) 8847–8851.
- [20] C.H. Yang, et al., Reduced leakage current, enhanced ferroelectric and dielectric properties in (Ce,Fe)-codoped Na<sub>0.5</sub>Bi<sub>0.5</sub>TiO<sub>3</sub> film, *Appl. Phys. Lett.* 100 (2012) 022909.
- [21] J. Yan, et al., Ferroelectric properties, morphologies, and leakage currents of Bi<sub>0.97</sub>La<sub>0.03</sub>FeO<sub>3</sub> thin films deposited on indium tin oxide/glass substrates, *J. Appl. Phys.* 104 (2008) 076103.
- [22] H. Zhang, et al., Large and uniform piezoresponse of BiFe<sub>0.995</sub>W<sub>0.005</sub>O<sub>3</sub> thin film annealed at 450 °C, *J. Mater. Sci.: Mater. Electron.* 23 (2012) 1864–1868.
- [23] Qingguo Chi, Jiefeng Dong, Highly (100)-oriented sandwich structure of (Na<sub>0.85</sub>K<sub>0.15</sub>)<sub>0.5</sub>Bi<sub>0.5</sub>TiO<sub>3</sub> composite films with outstanding pyroelectric properties, *J. Mater. Chem. C* (2016) 4442–4450.
- [24] Q.G. Chi, et al., Interface optimization and electrical properties of 0.5Ba(Zr<sub>0.2</sub>Ti<sub>0.8</sub>)O<sub>3</sub>-0.5(Ba<sub>0.7</sub>Ca<sub>0.3</sub>)TiO<sub>3</sub> thin films prepared by a sol-gel process, *J. Phys. Chem. C* 118 (2014) 15220–15225.
- [25] Q.G. Chi, et al., Enhanced performance of Pb<sub>0.8</sub>La<sub>0.1</sub>Ca<sub>0.1</sub>Ti<sub>0.975</sub>O<sub>3</sub>/Pb(Nb<sub>0.01</sub>Zr<sub>0.2</sub>Ti<sub>0.8</sub>)O<sub>3</sub> multilayer thin films for pyroelectric applications, *Appl. Phys. Lett.* 98 (2011) 242903.